

Quasispin model for itinerant magnetism—effects of short-range order

S. H. Liu

Ames Laboratory—Department of Energy and Department of Physics, Iowa State University, Ames, Iowa 50011

(Received 3 October 1977; revised manuscript received 12 December 1977)

The cluster-Bethe-lattice method has been used to study the short-range-ordered state of an itinerant magnetic system. We assume a local moment on each lattice site, but the moments may point up or down and have long- or short-range order. The electronic structure is solved, and the size of the local moments is determined self-consistently. It is found that the Friedel criterion for local moments in the disordered state is different from the Stoner criterion for ferromagnetic state. The phase transition from the ordered state to the paramagnetic state is, in most cases, described by a transition to the local-moment state with short-range order. In the disordered state the energy bands remain spin split over a large part of the wave-vector space. The wave vectors are complex due to spin disorder, and the electron wave function is a mixture of majority and minority band states.

I. INTRODUCTION

In the Stoner theory of itinerant magnetism the paramagnetic phase of the system is described as consisting of spin-degenerate electron bands. This description has been questioned by many authors in recent years. Moriya¹ and his co-workers have pointed out that the Stoner paramagnetic state underestimates the entropy of the system, and consequently overestimates the critical temperature. When they take into account localized spin fluctuations, they obtain a much-reduced critical temperature, a good Curie-Weiss temperature dependence for the static susceptibility, and a good description of the spin dynamics in the paramagnetic phase. Therefore, it appears to be essential to consider short-range spin fluctuations in the theory of weak itinerant ferromagnets.

Roth² and the present author³ have studied the condition under which magnetic moments may be localized in the Friedel-Anderson sense in the paramagnetic phase of an itinerant magnet. The basic idea of their calculation is as follows. The kinetic energy of the conduction electrons is measured by the width of the d band, which is approximately 2 eV for 3d transition metals. The kinetic energy of the spin motion is measured by kT_C , where T_C is the magnetic ordering temperature. Taking $T_C \cong 1000$ K as a typical value, one finds $kT_C \cong 0.1$ eV, which is much smaller than the electron bandwidth. Consequently, for the purpose of discussing the electronic structure, one can make the Born-Oppenheimer approximation and treat the spins as a set of local moments that are frozen in a randomly oriented pattern. To simplify the calculation further, the local moments are assumed to be Ising-like, i.e., they can only point up or down along a specified direction. Then the problem becomes identical to the random-binary-alloy

problem with the additional condition that the exchange potential must be tied self-consistently to the size of the local moment. Just like the single-impurity problem, the authors showed that the assumed spin structure could exist for a narrow enough band and strong enough Coulomb repulsion. They offered this spin structure as the description of the paramagnetic phase of strongly coupled itinerant magnets such as Fe, Co, and Ni. This view enjoys the support of the recent photoemission study on Ni,⁴ for which the photoemission spectrum is found to be insensitive to the magnetic ordering, indicating that there is essentially no change in the spin-split energy-level structure when the system undergoes order-disorder phase transition.

In Refs. 2 and 3 the paramagnetic phase is assumed to be a structure of completely random spins. This was done in order to apply the coherent-potential-approximation (CPA) method to solve for the local electronic structure. However, it is well established that in itinerant ferromagnets there is a great deal of short-range order just above the critical temperature.⁵ Therefore, the description of the disordered phase by a random-binary-alloy analogy is not entirely realistic. In this paper we study the effects of short-range order on the localization of the magnetic moments. Although methods have been developed recently to incorporate short-range order into the CPA formalism,⁶ we have found it more convenient to study the problem from a real-space approach proposed by Sen and Yndurain for binary alloys with short-range order.^{7,8} To make the problem tractable we restrict the spin direction to be either up or down along a fixed axis in space. We also take the size of the local moment to be the same on every site, and obtain a self-consistent equation which gives the dependence of the size of the local moment on the bandwidth, interaction strength, and the degree

of short-range order. We can include ferromagnetic and classical antiferromagnetic ground states as special limits when the range of ordering approaches infinity, but we cannot treat the helical spin state and the spin-density-wave state by this calculation. Since the main goal of this work is to discuss the electronic properties of the disordered phase, we feel that even with these restrictions it still represents a significant step toward a realistic theory.

II. METHOD OF SOLUTION

We represent the system by the single-band Hubbard model defined by the following Hamiltonian⁹:

$$H = -t \sum_{i\delta\sigma} (c_{i\delta\sigma}^\dagger c_{i,\sigma} + \text{H.c.}) + U \sum_i n_{i\uparrow} n_{i\downarrow}, \quad (2.1)$$

where t is the hopping integral, U is the Coulomb integral, the sum on i is over the lattice sites, the sum on δ is over the nearest neighbors of site i , and the sum on σ is over the spin states of the electrons. The number of nearest neighbors of a given site is denoted by Z .

The first step in the solution is to replace the last term of the Hamiltonian by a site- and spin-dependent potential. This approximation, originally suggested by Hubbard,⁹ has been extensively used by many authors.¹⁰⁻¹⁵ For a spin-up site we take $V_{i\sigma} = \frac{1}{2}Un - \sigma\Delta$, where Δ is the product of U and the size of the local moment, and n is the average number of electrons per site. For a spin-down site, the spin-dependent part of the potential has the opposite sign. In subsequent discussions the zero-energy level is redefined to remove the spin-independent part of the effective potential. The size of the local moment, assumed to be the same on every site, is to be determined self-consistently. We may distinguish between two broad kinds of magnetic states: (i) the Pauli state in which $\Delta = 0$ on every site; and (ii) the local moment state in which $\Delta \neq 0$. The Pauli state will be shown to be distinct from the disordered local-moment state, although they are both paramagnetic.

Following the formalism in Refs. 7 and 8 we write the equation for the local electron Green's function of a spin-up site

$$(\omega + \sigma\Delta)G_{i\sigma}(\omega) = 1 - t \sum_{\delta} G_{i+\delta, i, \sigma}(\omega). \quad (2.2)$$

Among the Z nearest neighbors of i there are Z' neighbors in spin-up state and $Z - Z'$ neighbors in spin-down state. We define the following transfer functions:

$$T_{\sigma}^{(\pm, +)} = G_{i+\delta, i, \sigma}(\omega) / G_{i\sigma}(\omega), \quad (2.3)$$

depending on whether the moment on site $i + \delta$ is

up or down. Then we can solve for the Green's function in terms of the transfer functions:

$$G_{i\sigma}(\omega) = [\omega + \sigma\Delta + Z'tT_{\sigma}^{(+, +)} + (Z - Z')tT_{\sigma}^{(+, -)}]^{-1}. \quad (2.4)$$

Similarly, for a spin-down site which has Z'' nearest neighbors in spin-down state, we have

$$G_{i\sigma}(\omega) = [\omega + \sigma\Delta + Z''tT_{\sigma}^{(-, -)} + (Z - Z'')tT_{\sigma}^{(-, +)}]^{-1}, \quad (2.5)$$

where the transfer functions $T_{\sigma}^{(\pm, \mp)}$ are defined in analogy with Eq. (2.3).

The equations for the transfer functions are derived from studying the equation of motion of $G_{i+\delta, i, \sigma}(\omega)$. Assuming that both sites i and $i + \delta$ are spin-up sites, and of the Z nearest neighbors of $i + \delta$ there are Z_1 in spin-up state and $Z - Z_1$ in spin-down state, then

$$(\omega + \sigma\Delta)T_{\sigma}^{(+, +)} = -t - t(Z_1 - 1)(T_{\sigma}^{(+, +)})^2 - t(Z - Z_1)T_{\sigma}^{(+, -)}T_{\sigma}^{(+, +)}. \quad (2.6)$$

Similarly, if i is spin-up but $i + \delta$ is spin-down, we find

$$(\omega - \sigma\Delta)T_{\sigma}^{(+, -)} = -t - t(Z - Z_2)T_{\sigma}^{(-, -)}T_{\sigma}^{(+, -)} - t(Z_2 - 1)T_{\sigma}^{(+, -)}T_{\sigma}^{(+, -)}, \quad (2.7)$$

where Z_2 is the number of nearest neighbors of $i + \delta$ that are in spin-up state. An essential approximation has been made at this point, namely, that the transfer functions defined in Eq. (2.3) are independent of the position of the site i . The validity of this step requires that the lattice branches out indefinitely without forming closed loops, and that each site is surrounded by an average environment which depends only on the spin direction of that site. The first requirement means that we approximate the real lattice by a Cayley tree or Bethe lattice.¹⁶ The second requirement is met rigorously only when the moments are ordered. In the disordered phase the average environment is realized after making suitable configurational averages.

Following the original work of Bethe on the short-range order in binary alloys,¹⁷ we denote by r the probability that a nearest neighbor of a site i has its local moment parallel to that of i , then $r = 1$ is the ferrromagnetic state, $r = 0$ is the anti-ferromagnetic state, $r = \frac{1}{2}$ is the random spin state, and all other values of r characterize short-range order. After averaging over configurations, Eqs. (2.4) and (2.5) become

$$G_{i\sigma}(\omega) = (\omega + \sigma\Delta + rZtT_{\sigma}^{(+, +)} + sZtT_{\sigma}^{(+, -)})^{-1} \quad (2.8)$$

for a spin-up site, and

$$G_{i\delta}(\omega) = (\omega - \sigma\Delta + rZtT_{\sigma}^{(-)} + sZtT_{\sigma}^{(+)})^{-1} \quad (2.9)$$

for a spin-down site. Here we have abbreviated $(1-r)$ by s .

The configuration averaging of the equations for the transfer functions is more subtle. For instance, Eqs. (2.6) and (2.7) should be averaged over only those configurations in which at least one nearest neighbor of $i+\delta$ is spin-up. Therefore,

$$\begin{aligned} \langle Z_1 - 1 \rangle &= \sum_{Z_1=1}^Z \binom{Z}{Z_1} r^{Z_1} s^{Z-Z_1} (Z_1 - 1) \\ &\quad \times \left[\sum_{Z_1=1}^Z \binom{Z}{Z_1} r^{Z_1} s^{Z-Z_1} \right]^{-1} \\ &= \frac{Zr + s^Z - 1}{1 - s^Z} \equiv Z_A, \end{aligned} \quad (2.10)$$

$$\langle Z - Z_1 \rangle = Z(s - s^Z)/(1 - s^Z) \equiv Z_B,$$

$$\langle Z - Z_2 \rangle = Z(r - r^Z)/(1 - r^Z) \equiv Z_C,$$

$$\langle Z_2 - 1 \rangle = (Zs + r^Z - 1)/(1 - r^Z) \equiv Z_D.$$

The complete set of equations for the transfer functions are

$$\begin{aligned} (\omega + \sigma\Delta)T_{\sigma}^{(+)} &= -t - tZ_A(T_{\sigma}^{(+)})^2 - tZ_B T_{\sigma}^{(+)} T_{\sigma}^{(+)}, \\ (\omega - \sigma\Delta)T_{\sigma}^{(-)} &= -t - tZ_C T_{\sigma}^{(-)} T_{\sigma}^{(-)} - tZ_D T_{\sigma}^{(-)} T_{\sigma}^{(-)}, \\ (\omega - \sigma\Delta)T_{\sigma}^{(-)} &= -t - tZ_A(T_{\sigma}^{(-)})^2 - tZ_B T_{\sigma}^{(-)} T_{\sigma}^{(-)}, \\ (\omega + \sigma\Delta)T_{\sigma}^{(+)} &= -t - tZ_C T_{\sigma}^{(+)} T_{\sigma}^{(+)} - tZ_D T_{\sigma}^{(+)} T_{\sigma}^{(+)}. \end{aligned} \quad (2.11)$$

In actual calculations these equations are solved and the results put into Eqs. (2.8) and (2.9) for the local Green's functions.

The local densities of states are determined from

$$D_{\sigma}(\omega) = -(1/\pi) \text{Im}G_{i\delta}(\omega). \quad (2.12)$$

The average number of electrons per site is

$$n = \int_{-\infty}^{\mu} [D_+(\omega) + D_-(\omega)] d\omega, \quad (2.13)$$

which relates the Fermi energy to the occupation number, and the size of the local moment per site is

$$S = \int_{-\infty}^{\mu} |D_+(\omega) - D_-(\omega)| d\omega. \quad (2.14)$$

To complete the self-consistency loop we relate the local exchange splitting to the local moment by $\Delta = US$. In the above two equations we have left out the temperature-dependent Fermi distribution function because in most itinerant magnetic materials the ordering temperature is much lower than the Fermi temperature of the electrons.

Before we proceed with the solution of the

coupled equations for the transfer functions we write down the results for three simple cases for later reference. In the Pauli paramagnetic state $\Delta = 0$ all the transfer functions reduce to one:

$$T_0 = \{-\omega + i[4(Z-1)t^2 - \omega^2]^{1/2}\}/2(Z-1)t. \quad (2.15)$$

The electron band is confined in the energy region where T_0 is complex, or $|\omega| \leq 2t(Z-1)^{1/2}$.^{7,8} The density of states for each spin is found to be

$$D(\omega) = \frac{Z}{2\pi} \frac{[4(Z-1)t^2 - \omega^2]^{1/2}}{Z^2 t^2 - \omega^2}. \quad (2.16)$$

In the ferromagnetic phase, $r=1, \Delta \neq 0$, there are two different transfer functions

$$T_{\pm} = T_{\pm}^{(+)} = \frac{-(\omega \pm \Delta) + i[4(Z-1)t^2 - (\omega \pm \Delta)^2]^{1/2}}{2(Z-1)t}. \quad (2.17)$$

All other transfer functions are undefined. The energy bands are rigidly split by 2Δ , and there is a local moment on each site as long as $n \neq 0$ or 2 .

In the limit of $\Delta \rightarrow 0$, the equation for the local moment, Eq. (2.14), reduces to $1 = UD(\mu)$, where $D(\mu)$ is the density of the unpolarized band at the Fermi level as determined from Eq. (2.16).

Therefore, the criterion for ferromagnetism is the familiar Stoner criterion $UD(\mu) > 1$.

In the antiferromagnetic phase, $r=0, \Delta \neq 0$, there are two distinct transfer functions

$$T_+^{(+)} = T_-^{(+)} = T_1, \quad T_+^{(-)} = T_-^{(-)} = T_2,$$

where

$$T_1 = \frac{-(\omega^2 - \Delta^2) + i[4(Z-1)t^2(\omega^2 - \Delta^2) - (\omega^2 - \Delta^2)^2]^{1/2}}{2t(Z-1)(\omega - \Delta)},$$

$$T_2 = [(\omega - \Delta)/(\omega + \Delta)]T_1. \quad (2.18)$$

The energy bands are bounded by

$$\Delta \leq |\omega| \leq [\Delta^2 + 4(Z-1)t^2]^{1/2}. \quad (2.19)$$

There is an energy gap of the size 2Δ in the middle of the band. For a half-filled band ($n=1$) in the weak coupling limit, the energy gap is related to the coupling constant U by

$$\Delta \cong 4E_B \exp[-1/ZUD(0)], \quad (2.20)$$

where $E_B = 2t(Z-1)^{1/2}$, $D(0) = (Z-1)^{1/2}/\pi Zt$. This result is quite similar to that of the Fedders-Martin theory of itinerant antiferromagnetism¹⁸

$$\Delta = 4t \exp[-1/UD(0)].$$

The differences between the two results come partly from the difference in the band models and partly from the Bethe-lattice approximation.

Next, we consider the disordered phase in the limit of small Δ . This determines the phase boundary between the Pauli state and the local-mo-

ment state, thereby giving the generalization of the Friedel criterion. In this case all transfer functions differ from T_0 by quantities of the order of Δ , so the coupled equations may be linearized and solved for the deviations. After a straightforward but tedious calculation we find the stability criterion for the local-moment state to be $U > U_c$, where

$$U_c^{-1} = \frac{1}{4\pi} \int_{-\infty}^{\mu} \text{Im} \frac{1 - ZrtA + ZstB}{(\omega + ZtT_0)^2} d\omega \quad (2.21)$$

and

$$\begin{aligned} A &= T_0[\omega + (Z-1)tT_0 - (Z_D - Z_B)tT_0]/D, \\ B &= T_0[\omega + (Z-1)tT_0 - (Z_C - Z_A)tT_0]/D, \\ D &= [\omega + (Z-1)tT_0 + Z_A tT_0] \\ &\quad \times [\omega + (Z-1)tT_0 - Z_D tT_0] + Z_B Z_C t^2 T_0^2. \end{aligned} \quad (2.22)$$

The result of the calculation of U_c as a function of the short-range order parameter r is summarized in Fig. 1. The abscissa is the occupation number n in the range $0 \leq n \leq 1$, and the ordinate is the interaction strength U normalized by the bandwidth E_B . Due to the complete particle-hole symmetry, the part of the graph for $1 \leq n \leq 2$ can be obtained

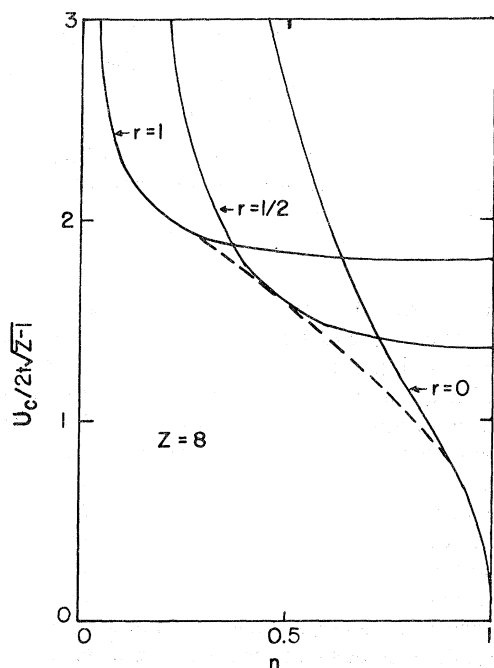


FIG. 1. Critical interaction U_c which stabilizes a local-moment state with short-range order parameter r , plotted as a function of r and average electron occupation number n . The dotted curve marks the phase boundary between the Pauli state and the local-moment state with the lowest U_c .

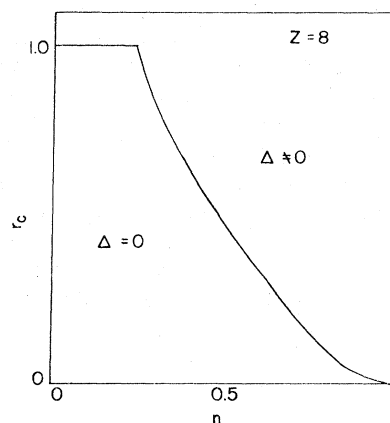


FIG. 2. Critical short-range parameter r_c corresponding to the local-moment state of lowest U_c , plotted as a function of the average electron occupation.

by reflecting Fig. 1 along the $n=1$ line. The three curves labeled by $r=1$, $r=0$, and $r=\frac{1}{2}$ represent the critical interaction strength for ferromagnetic, antiferromagnetic, and random spin states, respectively. The dotted curve which envelopes the U_c curves marks the phase boundary between the Pauli state and the local-moment state which has the lowest U_c . The corresponding short-range order parameter r_c is plotted as a function of the occupation number in Fig. 2.

The two graphs Figs. 1 and 2 point out that the generalized Friedel criterion for local moments in the disordered state is different from the Stoner criterion for ferromagnetic state.¹⁹ This result is in qualitative agreement with that of the CPA study.^{2,20} For $n=1$ the antiferromagnetic state is stable for an infinitesimal value of U . For small values of n the system transforms from the Pauli state to the ferromagnetic state when the interaction strength is increased beyond the critical value U_c . For a wide intermediate range of n the first local-moment state that becomes stable upon increasing U has short-range order.

III. PROPERTIES OF THE LOCAL-MOMENT STATES

When $\Delta \neq 0$ we must solve the full set of coupled nonlinear equations for the eight transfer functions. With suitable transformations the equations may be solved by first solving an algebraic equation of degree 8, and the solution of physical interest is one of the complex roots. There exists no algorithm which allows this root to be picked out automatically. Therefore, we have devised a simplifying approximation which reduces the task of numerical analysis significantly without sacrificing accuracy. The approximation is made when we

average the equations for the transfer functions over configurations. For example, consider the equation for $T_{\sigma}^{(++)}$, Eq. (2.6). The equation is derived under the condition that the sites i and $i+\delta$ are both spin-up. The other $Z-1$ nearest neighbors of $i+\delta$ are assumed to have independent probabilities of being in up or down state, and these probabilities are r and s , respectively. The averaged equations for the transfer functions have the same form as Eq. (2.11) except that

$$Z_A = Z_C = r(Z-1), \quad Z_B = Z_D = s(Z-1). \quad (3.1)$$

We define

$$\eta_{\sigma} = rT_{\sigma}^{(++)} + sT_{\sigma}^{(-+)}, \quad \zeta_{\sigma} = rT_{\sigma}^{(--)} + sT_{\sigma}^{(+-)}, \quad (3.2)$$

then we can express all the transfer functions in terms of η_{σ} and ζ_{σ} ;

$$T_{\sigma}^{(++)} = -t/[\omega + \sigma\Delta + t(Z-1)\eta_{\sigma}], \quad (3.3)$$

$$T_{\sigma}^{(-+)} = -t/[\omega - \sigma\Delta + t(Z-1)\zeta_{\sigma}],$$

etc. Furthermore, the equations for η_{σ} and ζ_{σ} are

$$-\eta_{\sigma} = \frac{rt}{\omega + \sigma\Delta + t(Z-1)\eta_{\sigma}} + \frac{st}{\omega - \sigma\Delta + t(Z-1)\zeta_{\sigma}},$$

$$-\zeta_{\sigma} = \frac{rt}{\omega - \sigma\Delta + t(Z-1)\zeta_{\sigma}} + \frac{st}{\omega + \sigma\Delta + t(Z-1)\eta_{\sigma}}. \quad (3.4)$$

There is also the symmetry relation

$$\eta_{\sigma} = \zeta_{-\sigma}. \quad (3.5)$$

By eliminating either η_{σ} or ζ_{σ} from the coupled equations, we obtain a quartic equation which in general has two pairs of complex roots. The roots can be determined by the well-known algorithm for solving quartic equations, and the root of physical interest can be picked out as the one which satisfies the original coupled equations and has the correct analytic property.

We have tested the accuracy of this approximate averaging scheme by comparing the critical interaction parameter U_c calculated this way with that determined in Sec. II. It is obvious that for $r=0$ or 1 the two averaging methods are identical. For intermediate values of r the U_c curves differ by less than 5% for $Z=6$, and 1% for $Z=12$. We are, therefore, confident that the simple averaging scheme should give results which are very close to those given by the more rigorous scheme. In addition all the physical quantities can be calculated with great precision. This allows us to compare the energies of local-moment states with slightly different degrees of short-range order.

In Fig. 3 we show the result for the local densities of states of the short-range ordered state and

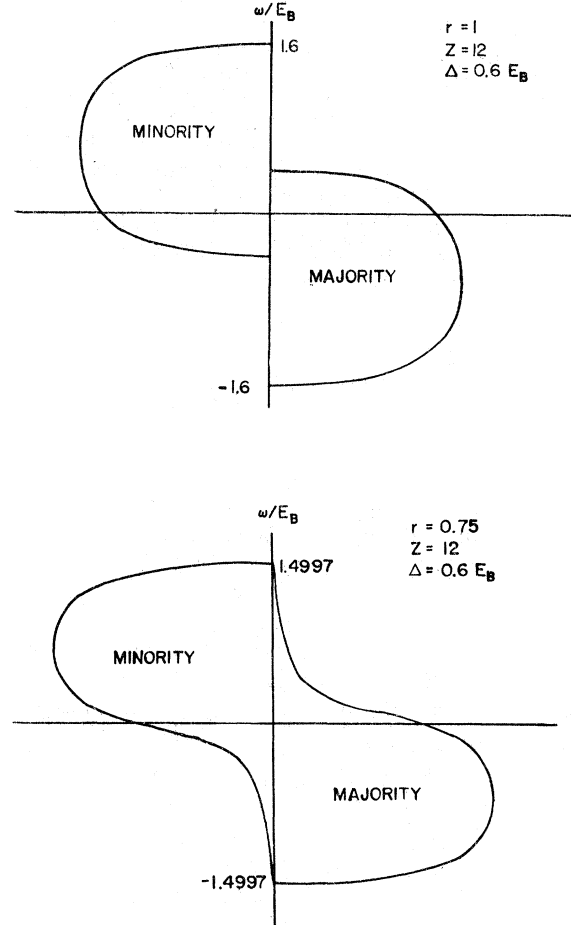


FIG. 3. Local densities of states of the ferromagnetic state (top) and the disordered local-moment state (bottom).

compare them with those of the ferromagnetic state. The major differences are that in the disordered state the energy levels spread out over a wider range of energy while the main peaks of the densities of states are narrower. Both features can be understood from a consideration of the motion of the electrons through the lattice. In the disordered state an electron must travel among sites of opposite spin directions, thereby experiencing a fluctuation of the Coulomb potential. This makes the overall bandwidth larger. However, the hopping of an electron between sites of opposite spins is not as easy as that between sites of parallel spins, so the electron prefers to travel among sites of parallel spins. In the disordered state there is a decrease in the number of parallel spin nearest-neighbor sites, and consequently the high-density part of the bands become narrower.

For the one-dimensional case ($Z=2$) the equa-

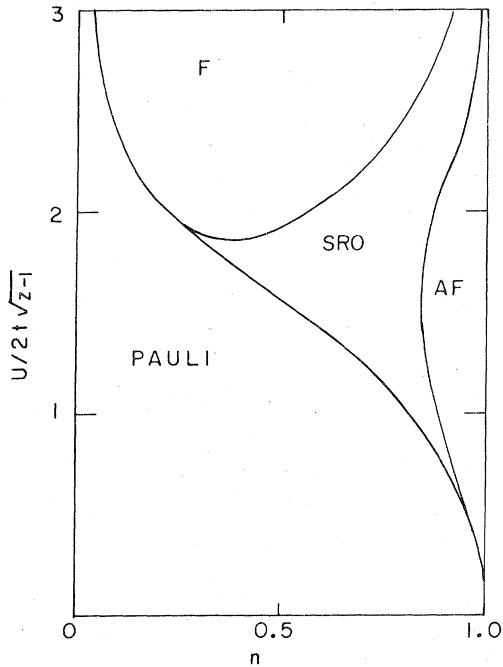


FIG. 4. Phase diagram of the itinerant magnetic system according to the cluster-Bethe-lattice calculation. SRO indicates the short-range-ordered local-moment state.

tions of the transfer functions also have real roots corresponding to local states. Unlike the calculations of Refs. 7 and 8 the simple averaging scheme we have used does not give local states for $Z > 2$.

The internal energy per site is given by

$$E = \frac{1}{4} Un^2 + \int_{-\infty}^{\mu} [(\omega + \frac{1}{2}\Delta)D_+(\omega) + (\omega - \frac{1}{2}\Delta)D_-(\omega)] d\omega, \quad (3.6)$$

where we have reinserted the spin-independent part of the Coulomb interaction. For fixed values of U and n we choose a value of r and solve the equations self-consistently for Δ . The most stable configuration for the set of U and n is found by minimizing E with respect to r . This enables the determination of the phase diagram in Fig. 4, which is computed for $Z = 12$ in order to minimize the error due to the simple averaging scheme. Again the phase diagram is only drawn for $0 \leq n \leq 1$. The part for $1 \leq n \leq 2$ may be inferred from particle-hole symmetry.

The following features of the phase diagram are worth discussing. In the large U limit we find that the preferred spin ordering is ferromagnetic except when $n = 1$. This result agrees with the conclusion of Nagaoka²¹ and others.²²⁻²⁴ For very small values of n the system makes a transition

from the Pauli state to the ferromagnetic state when U is increased, in agreement with the Stoner theory of ferromagnetism. However, for a wide range of intermediate values of n and U our theory differs from the Stoner theory in that it predicts a disordered local-moment state to be more stable than both the Pauli state and the ferromagnetic state. The Stoner theory is based on a band Hartree-Fock approximation, so it precludes from consideration any state of disordered local moments. Our theory, which is based on a local Hartree-Fock approximation, includes such states and predicts that they are rather important. By the same argument our theory is limited by the constraints mentioned in Sec. I, so it may preclude from consideration other types of states with even lower energy than the disordered local-moment state. Therefore, the phase diagram definitely does not imply that the ground state of the system is a state of short-range order.

Penn studied the stability of a number of magnetically ordered states and the paramagnetic local-moment state in the one-band Hubbard model.²⁵ His phase boundary for stable paramagnetic local-moment state is virtually identical to our $r = \frac{1}{2}$ curve in Fig. 1. Since he did not consider local moments with short-range order, he could not have obtained the phase boundary between the Pauli state and the local-moment state as shown by the dashed curve in Fig. 1. Nevertheless, this particular phase boundary has close similarity with Penn's stability criterion for ordered magnetic states. We can not describe the special ferromagnetic state of Penn in our calculation. This state is identical to the antiferromagnetic state for $n = 1$, and the stability of this state is reproduced by our calculation. For $n \neq 1$ our short-range order state represents the best we can do to mimic either the helical-spin-density-wave state or the special ferrimagnetic state.

The energy calculation allows us to estimate the Curie temperature of the spin system. In the Weiss theory the molecular field parameter λ is twice the energy difference per site between the fully ordered phase ($r = 1$) and the totally random state ($r = \frac{1}{2}$), i.e.,

$$E(r = \frac{1}{2}) - E(r = 1) = \frac{1}{2}\lambda. \quad (3.7)$$

On the phase diagram in Fig. 4, λ is positive above the phase boundary between short-range order (SRO) and F . The mean-field approximation stipulates that in the partially ordered phase for which the relative magnetization per site is m ($0 \leq m \leq 1$), the internal energy is

$$E(m) - E(r = 1) = \frac{1}{2}\lambda(1 - m^2). \quad (3.8)$$

The entropy of the partially ordered state is

$$S(m) = -k \left[\left(\frac{1+m}{2} \right) \ln \left(\frac{1+m}{2} \right) + \left(\frac{1-m}{2} \right) \ln \left(\frac{1-m}{2} \right) \right]. \quad (3.9)$$

The entropy of the fully ordered state is zero. Minimizing the free energy ($E - TS$) with respect to m gives the familiar results

$$m = \tanh(\lambda m / kT), \quad (3.10)$$

and the Curie temperature

$$kT_C = \lambda. \quad (3.11)$$

In Fig. 5 we show the dependence of the Curie temperature on the bandwidth and U for $n=0.6$, a number representative of Ni. We find that for a wide range of U , $kT_C \cong 0.04 E_B \cong 0.08$ eV for $E_B \cong 2$ eV. This gives $T_C \cong 1000$ K, which is of the correct order of magnitude. We hasten to emphasize that this is a very crude estimate. In view of the over-simplified band model and the Ising approximation for the local moments, we see no point in trying to improve the estimate by using more sophisticated theories of phase transition.

At a temperature comparable to the level splitting Δ , the local moments must dissolve away as shown by Langer *et al.*²⁶ We have not studied the temperature dependence of the local moment. However, we may estimate the order of magnitude of the temperature T_M for stable local moments by

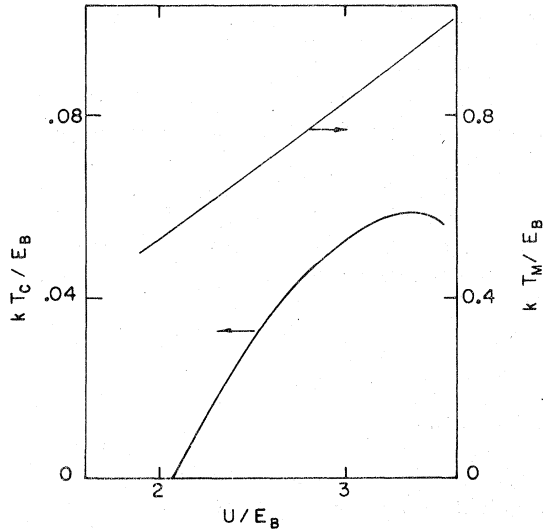


FIG. 5. Curie temperature T_C and the moment localization temperature T_M as functions of U and bandwidth E_B for a ferromagnetic system with $n=0.6$. For $U/E_B > 3.5$, T_C decreased slowly with increasing U .

$kT_M = \Delta$. Above T_M the Pauli state is obtained. It is shown in Fig. 5. that $T_C \cong 0.1 T_M$. That T_C is so much smaller than T_M is partly due to the fact that the local moments carry a much larger entropy than the degenerate electron gas as pointed out by Moriya,¹ and partly due to the fact that the energy required to change the spin alignment is much smaller than the energy involved in localizing the moments. This conclusion is in complete accord with that of Langer *et al.*²⁶ for the antiferromagnetic ($n=1$) case.

IV. ENERGY BANDS IN THE DISORDERED STATE

We will show in this section that the cluster-Bethe-lattice method can be used to investigate the band structure of the itinerant magnet in the disordered phase. We first illustrate the method by considering the ferromagnetic state. We study the Green's function $G_{i+l,i,\sigma}(\omega)$ for which the initial and final electrons are separated by l steps. By definition of the transfer function the Green's function has the expression

$$G_{i+l,i,\sigma}(\omega) = T_\sigma^l G_{i\sigma}(\omega), \quad (4.1)$$

where T_σ is given by Eq. (2.17). Therefore, the transfer function determines a phase shift when the electron moves from one site to another, and can be related to the wave vector corresponding to the energy ω .

There is one complication which arises from the Bethe-lattice approximation. It can be verified that

$$|T_\sigma|^2 = (Z-1)^{-1}, \quad (4.2)$$

which means that T_σ introduces both a phase shift and an amplitude factor. The latter appears because the Bethe-lattice branches out indefinitely with $Z-1$ new branches coming out of every lattice point. The electron density is correspondingly diluted whenever the electron moves down the lattice by one step. We can correct for this effect by normalizing the transfer function T_σ by the factor $(Z-1)^{1/2}$. Then we can define the wave vector by

$$e^{ikl} = (Z-1)^{1/2} T_\sigma^l. \quad (4.3)$$

This gives the band dispersion relation

$$\omega \pm \Delta = -2t(Z-1)^{1/2} \cos k, \quad 0 \leq k \leq \pi. \quad (4.4)$$

The energy bands are plotted in Fig. 6.

In the disordered phase the Green's function can be generated from a set of recurrent relations. If $(i+l)$ is a spin-up site, then the Green's function $G_{i+l,i,\sigma}^{(+)}(\omega)$ is related to $G_{i+l-1,i,\sigma}(\omega)$ by either $T_\sigma^{(++)}$ or $T_\sigma^{(+-)}$ depending on whether the site $(i+l-1)$ is spin-up or spin-down. Therefore

$$G_{i+l,i,\sigma}^{(+)}(\omega) = rT_{\sigma}^{(+)}G_{i+l-1,i,\sigma}^{(+)}(\omega) + sT_{\sigma}^{(-)}G_{i+l-1,i,\sigma}^{(-)}(\omega). \quad (4.5)$$

Similarly, if the site $(i+l)$ is spin-down, we find

$$G_{i+l,i,\sigma}^{(-)}(\omega) = rT_{\sigma}^{(-)}G_{i+l-1,i,\sigma}^{(-)}(\omega) + sT_{\sigma}^{(+)}G_{i+l-1,i,\sigma}^{(+)}(\omega). \quad (4.6)$$

The general solution of these difference equations is

$$G_{i+l,i,\sigma}^{(\pm)}(\omega) = A^{(\pm)}(Z-1)^{-l/2}e^{ik_1l} + B^{(\pm)}(Z-1)^{-l/2}e^{ik_2l}, \quad (4.7)$$

where $A^{(\pm)}$, $B^{(\pm)}$ are determined by the initial conditions, and the factor $(Z-1)^{-l/2}$ has been inserted at the appropriate places to account for the dilution effect. The phase factors are explicitly given by

$$e^{ik_1}, e^{ik_2} = \frac{1}{2}(Z-1)^{1/2} \left\{ r(T_{\sigma}^{(+)} + T_{\sigma}^{(-)}) \pm [r^2(T_{\sigma}^{(+)} - T_{\sigma}^{(-)})^2 + 4s^2T_{\sigma}^{(+)}T_{\sigma}^{(-)}]^{1/2} \right\}. \quad (4.8)$$

The dispersion relations are complex due to the scattering of the electrons from the disordered local moments.

In Fig. 6 we also show the energy bands for $r = 0.75$, $Z = 12$, and $\Delta = 0.6E_B$. The calculation was

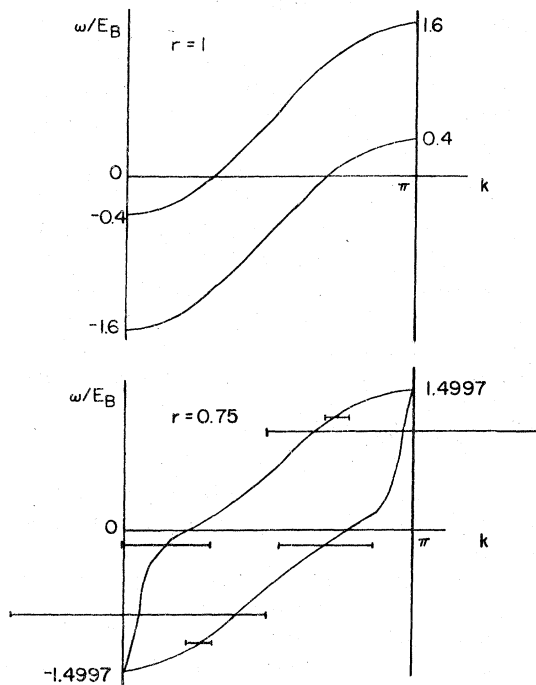


FIG. 6. Energy bands in the ferromagnetic state (top) and in the disordered state (bottom). The horizontal error bars indicate the natural linewidth of the electron level due to spin disorder scattering.

performed under the simplified averaging scheme in Sec. III. In the middle range of k the energy bands resemble those in the ordered phase in that the two bands are nearly parallel with a splitting very close to 2Δ . We may call the lower band the *majority spin band* and the upper band the *minority spin band*. An electron moving through the lattice spends some time in each band because it must travel across regions with opposite spin alignment. The electron mean free path is very close to the spin correlation length defined by

$$\Lambda = (-\ln|r-s|)^{-1}. \quad (4.9)$$

This is to be expected because spin correlation and electron correlation have the same physical meaning.

Near $k=0$ the majority band behaves normally with a relatively small linewidth, but the minority band makes a sharp turn downward accompanied by a large increase in linewidth. The explanation of this behavior is as follows. Consider a low-energy majority-band electron moving in a cluster of correlated sites. When this electron moves out of the cluster and enters a region where the sites reverse their spin direction, it must go into the minority band. This is possible only if the minority band dips down into the energy range of the majority band. Now this low-energy electron does not have enough kinetic energy to overcome the highly repulsive Coulomb correlation potential. Consequently it suffers a strong scattering back into the region where it is in an energetically favorable state. The fact that the electron cannot travel very far as a minority electron is the reason for the large linewidth of the band in the low-energy region. Similarly a hole near the top of the minority band must also be strongly scattered when it moves out of the cluster of correlated sites, and this gives rise to the anomalous behavior of the majority band near $k=\pi$. A different manifestation of this scattering effect was discussed earlier in connection with the shapes of the density-of-states curves in the disordered state.

Anderson showed that the electron states in disordered solids can be divided into two classes, the local states whose wave functions extend over a small region of the solid and the extended states whose wave functions thread through the solid.^{27,28} The Bethe lattice is topologically a one-dimensional lattice, so there are strictly speaking no extended states.²⁹ However, some vestige of the Anderson transition can be seen in the band structure of the disordered phase. The minority electron states near $k=0$ and the majority electron states near $k=\pi$ have large linewidths, so these are to be identified as local states. In the regions where the bands are normal, the linewidths are not nearly as

large, indicating a tendency for the electron wave function to spread out. The local states are necessary in our description of the disordered phase because they give rise to isolated down-up spins surrounded by a cluster of up-down spins.

The band structure explains the lack of sensitivity of the photo-emission spectrum of nickel when the temperature is raised above the Curie point.⁴ The finite life time of the electron is the origin of the large spin-disorder resistivity of nickel and iron.^{3,30}

V. APPLICATION TO ONE-DIMENSIONAL MODEL

We have used the cluster-Bethe-lattice method to calculate the ground-state energy of the one-dimensional model for the purpose of assessing the accuracy of the local Hartree-Fock approximation. The linear lattice is a Cayley tree, so the Bethe-lattice part of the method is exact. The exact ground-state energy of the Hubbard linear chain has been calculated by Lieb and Wu,³¹ so we can use their result as the standard for comparison.

In the linear-chain model we again find that for $n \neq 0$ or 1 the state of lowest energy is the short-range-ordered state. This is definitely wrong because it is well known that the ground state of the system is a helical spin-density-wave state for all values of the occupation number. The error occurs because we have restricted the direction of the local moments to be up or down along a fixed direction. There is only basis for comparison in the case of $n=1$ where the helical spin-density-wave state becomes the antiferromagnetic state.

The transfer functions for the antiferromagnetic state are given in Eq. (2.18). Putting these into the expressions for the Green's functions and taking the

imaginary parts, we obtain the densities of states for a spin-up site

$$D_{\pm}(\omega) = \frac{1}{\pi} \frac{(\omega^2 - \Delta^2)^{1/2}}{|\omega \pm \Delta| (\Gamma^2 - \omega^2)^{1/2}}, \quad (5.1)$$

where $\Gamma = (\Delta^2 + 4t^2)^{1/2}$. These results are used in Eq. (3.6) to calculate the ground-state energy per site. The Fermi energy is zero for the half-filled band. We obtain

$$E = \frac{1}{4}U - (2/\pi\Gamma) [\Gamma^2 E(2t/\Gamma) - \frac{1}{2} \Delta^2 K(2t/\Gamma)], \quad (5.2)$$

where $E(2t/\Gamma), K(2t/\Gamma)$ are complete elliptic integrals. The band splitting Δ is related to U by

$$1 = (U/\pi\Gamma)K(2t/\Gamma). \quad (5.3)$$

These relations enable us to plot E as a function of U as shown in Fig. 7. In the small U limit

$$E \cong -4t/\pi + \frac{1}{4}U, \quad (5.4)$$

and in the large U limit

$$E \cong -2t^2/U. \quad (5.5)$$

The exact E -vs- U curve is also plotted in Fig. 7 for comparison. In particular, in the small U limit our result agrees with the exact result up to the order U . In the large U limit the exact result is

$$E \cong -4t^2(\ln 2)/U = -2.77t^2/U. \quad (5.6)$$

Our result differs from this by 38%. The overall agreement between the two curves is reasonably good. Therefore, we conclude that the local Hartree-Fock approximation is a qualitatively sound method for the problem of itinerant magnetism for all values of U except in dealing with spin-density-wave and helical spin states.

VI. DISCUSSION

The work presented here adds further support to the idea that the paramagnetic phase of itinerant ferromagnets consists of disordered local moments, although the size of the quasispins is in general different from the saturation magnetization at low temperatures. This is a significant departure from the Stoner theory in which the paramagnetic phase is described by the Pauli state with spin-degenerate bands.

The quasispin model implies locally spin-split electron bands. Over the whole crystal the electron wave function is a mixture of both majority and minority band states and is strongly scattered. This introduces a new element in the study of the dynamics of the electrons.

There is definitely room for improvement in the present theory. We have only considered the average size of the quasispins and their average correlation. A complete theory must take into consideration the fluctuations both in the size and the or-

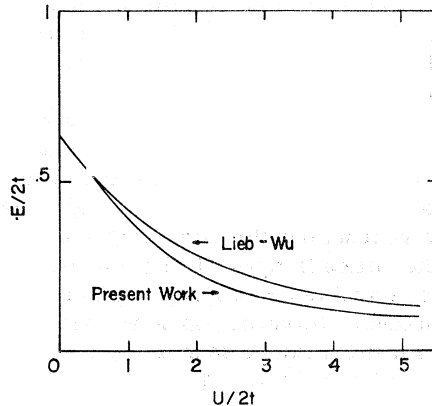


FIG. 7. Comparison of the ground-state energy of the one-dimensional model calculated by the Bethe-lattice method with the exact result of Lieb and Wu.

orientations of the quasispins. The size fluctuation may be introduced by the method of Moriya¹ except that the local susceptibility must be employed. One may study the orientation fluctuations by analogy with the Heisenberg model. The essential question of how the two types of fluctuations are coupled together and influence each other seems to be very difficult to resolve.

VII. ACKNOWLEDGMENTS

A part of this work was done when the author was visiting the Solid State Theory group at Berkeley. He wishes to thank Professor L. M. Falicov and his co-workers for illuminating discussions. This work was supported by the U. S. Dept. of Energy, Office of Basic Energy Sciences.

- ¹T. Moriya and A. Kawabata, *J. Phys. Soc. Jpn.* **34**, 639 (1973); **35**, 669 (1973); K. Ueda and T. Moriya, *ibid.* **39**, 605 (1975); T. Moriya, *ibid.* **40**, 933 (1976).
- ²L. Roth, in Proceedings of the Physics of Transition Metals Conference, Toronto, Canada, August 15–19, 1977 (unpublished).
- ³S. H. Liu, *Phys. Rev. B* **15**, 4281 (1977).
- ⁴L.-G. Petersson, R. Melander, D. P. Spears, and S. B. M. Hagström, *Phys. Rev. B* **14**, 4177 (1976).
- ⁵M. F. Collins, V. J. Minkiewicz, R. Nathans, L. Passell, and G. Shirane, *Phys. Rev.* **179**, 417 (1969); V. J. Minkiewicz, M. F. Collins, R. Nathans, and G. Shirane, *ibid.* **182**, 624 (1969).
- ⁶F. Brouers, M. Cyrot, and F. Cyrot-Lackman, *Phys. Rev. B* **7**, 4370 (1973), and references cited therein; W. H. Butler, *ibid.* **8**, 4499 (1973), and references cited therein.
- ⁷P. N. Sen and F. Yndurain, *Phys. Rev. B* **13**, 4387 (1976).
- ⁸R. C. Kittler and L. M. Falicov, *J. Phys. C* **9**, 4259 (1976), and references cited therein.
- ⁹J. Hubbard, *Proc. R. Soc. A* **276**, 238 (1963); **277**, 237 (1964); **281**, 401 (1964).
- ¹⁰M. Cyrot, *J. Phys. (Paris)* **33**, 125 (1972).
- ¹¹P. Lacour-Gayet and M. Cyrot, *J. Phys. C* **7**, 400 (1974).
- ¹²W. Langer, *J. Phys. C* **4**, L56 (1971).
- ¹³L. C. Bartel and H. S. Jarrett, *Phys. Rev. B* **10**, 946 (1974).
- ¹⁴W. Weller, *Phys. Status Solidi B* **54**, 611 (1972).
- ¹⁵E. N. Economou and C. T. White, *Phys. Rev. Lett.* **38**, 289 (1977).
- ¹⁶C. Domb, *Adv. Phys.* **9**, 149 (1960).
- ¹⁷H. A. Bethe, *Proc. R. Soc. A* **150**, 552 (1935).
- ¹⁸P. A. Fedders and P. C. Martin, *Phys. Rev.* **143**, 245 (1966).
- ¹⁹J. Friedel, G. Leman, and S. Olszewski, *J. Appl. Phys.* **32**, 325S (1961).
- ²⁰The result reported in Ref. 3 that the Friedel criterion is the same as Stoner criterion for the general band model is erroneous because the author did not use the correct local density of states for the magnetic-moment calculation.
- ²¹Y. Nagaoka, *Phys. Rev.* **147**, 392 (1966).
- ²²D. M. Edwards, *Proc. R. Soc. A* **300**, 373 (1967).
- ²³L. Roth, *Phys. Rev.* **186**, 428 (1969).
- ²⁴D. C. Mattis and R. E. Peña, *Phys. Rev. B* **10**, 1006 (1974).
- ²⁵D. R. Penn, *Phys. Rev.* **142**, 350 (1966).
- ²⁶W. Langer, M. Plischke and D. Mattis, *Phys. Rev. Lett.* **23**, 1448 (1969).
- ²⁷P. W. Anderson, *Phys. Rev.* **109**, 1492 (1958).
- ²⁸For a comprehensive review of the Anderson transition in disordered solids, see E. N. Economou, M. H. Cohen, K. F. Freed, and E. S. Kirkpatrick, in *Amorphous and Liquid Semiconductors*, edited by J. Tauc (Plenum, New York, 1974), pp. 101–158.
- ²⁹E. N. Economou and M. H. Cohen, *Phys. Rev. Lett.* **24**, 218 (1970).
- ³⁰T. Kasuya, *Prog. Theor. Phys.* **16**, 58 (1956).
- ³¹E. H. Lieb and F. Y. Wu, *Phys. Rev. Lett.* **20**, 1445 (1968).